Tryptophan-Anchored Transmembrane Peptides Promote Formation of Nonlamellar Phases in Phosphatidylethanolamine Model Membranes in a Mismatch-Dependent Manner†

Patrick C. A. van der Wel,‡ Tanja Pott,§ Sven Morein,|| Denise V. Greathouse,‡ Roger E. Koeppe II,*,‡ and J. Antoinette Killian*,||

Department of Chemistry and Biochemistry, University of Arkansas, Fayetteville, Arkansas 72701, Centre de Recherche Paul Pascal−CNRS, Av. A. Schweitzer, 33600 Pessac, France, and Department of Biochemistry of Membranes, Center for Biomembranes and Lipid Enzymology, Institute of Biomembranes, University of Utrecht, Padualaan 8, 3584 CH Utrecht, The Netherlands

Received September 28, 1999; Revised Manuscript Received December 30, 1999

ABSTRACT: To better understand the mutual interactions between lipids and membrane-spanning peptides, we investigated the effects of tryptophan-anchored hydrophobic peptides of various lengths on the phase behavior of 1,2-dielaidoylphosphatidylethanolamine (DEPE) dispersions, using ^{31}P nuclear magnetic resonance and small-angle X-ray diffraction. Designed α-helical transmembrane peptides (WALP*n* peptides, with *n* being the total number of amino acids) with a hydrophobic sequence of leucine and alanine of varying length, bordered at both ends by two tryptophan membrane anchors, were used as model peptides and were effective at low concentrations in DEPE. Incorporation of 2 mol % of relatively short peptides (WALP14−17) lowered the inverted hexagonal phase transition temperature (T_H) of DEPE, with an efficiency that seemed to be independent of the extent of hydrophobic mismatch. However, the tube diameter of the H_{II} phase induced by the peptides was clearly dependent on mismatch and decreased with shorter peptide length. Longer peptides (WALP19−27) induced a cubic phase, both below and above T_H. Incorporation of WALP27, which is significantly longer than the DEPE bilayer thickness, did not stabilize the bilayer. The longest peptide used, WALP31, hardly affected the lipid's phase behavior, and appeared not to incorporate into the bilayer. The consequences of hydrophobic mismatch between peptides and lipids are therefore more dramatic with shorter peptides. The data allow us to suggest a detailed molecular model of the mechanism by which these transmembrane peptides can affect lipid phase behavior.

Biological membranes act as permeability barriers, defining cells and intracellular compartments. The membrane lipids provide this permeability barrier by arranging themselves in a bilayer structure. However, biological membranes often also contain lipids that on their own do not form bilayers when dispersed under physiological conditions (*1*−*4*). Instead these lipids organize in nonlamellar structures, such as cubic phases or the inverted hexagonal (H_{II})[1] phase. We will refer to these lipids simply as nonbilayer lipids. Several organisms have been shown to regulate the amounts of bilayer and nonbilayer lipids, to maintain a certain nonbilayer-forming propensity in their membranes (*5*−*7*). This suggests that the presence of a certain amount of nonbilayer lipids is essential for structural and/or functional properties of the membrane.

Nonbilayer lipids are characterized by a smaller effective size of their headgroup compared to the area occupied by their acyl chains, resulting in a negative spontaneous monolayer curvature (*4, 8*). A possible rationale for the importance of nonbilayer lipids is that their presence in membranes causes a curvature stress, which affects lipid packing and/or changes the pressure exerted by the lipids on membrane proteins (*9*−*11*). This could modify the conformation, and therefore the activity, of these proteins. Indeed, it has been shown that nonbilayer lipids can influence the activity of a number of membrane proteins. Examples are the gating of the channel-forming peptide alamethicin (*12*); the activity of protein kinase C (*13*), ubiquinol−cytochrome *c* reductase and mitochondrial H^+-ATPase (*14*), insulin receptor (*15*), Ca^{2+}-ATPase (*16, 17*), and rhodopsin (*18*); and the ATPase activity of SecA (*19*).

Alternatively, it has been proposed that the ability of the lipids to form nonlamellar phases may be important for functional membrane processes, which require local and transient deviation from the bilayer (*20, 21*). An example is

† This work was supported in part by Grant GM-34968 from the NIH, by NATO Grant CRG 950357, and by EU TMR Network Grant ERBFMRX CT96 0004.

* To whom correspondence should be addressed at (R.E.K.) the University of Arkansas (phone: 501-575-4976, fax: 501-575-4049, e-mail: rk2@uafsysb.uark.edu) or (J.A.K.) the University of Utrecht (phone: +31-30-2533442, fax: +31-30-2522478, e-mail: j.a.killian@chem.uu.nl).

‡ University of Arkansas.

§ Centre de Recherche Paul Pascal−CNRS.

|| University of Utrecht.

[1] Abbreviations: NMR, nuclear magnetic resonance; L_α, lamellar liquid crystalline; L_β, lamellar gel; H_{II}, inverted hexagonal; DEPE, 1,2-dielaidoylphosphatidylethanolamine; DOPE, 1,2-dioleoylphosphatidylethanolamine; PC, phosphatidylcholine; TFA, trifluoroacetic acid; TFE, 2,2,2-trifluoroethanol; T_L, gel to liquid-crystalline phase transition temperature; T_H, lamellar liquid-crystalline to inverted hexagonal phase transition temperature.

10.1021/bi9922594 CCC: $19.00
Published on Web 02/25/2000

membrane fusion (*22*). Since protein−lipid interactions are likely to be involved in such processes and since it is known that proteins can affect lipid phase behavior (for a review, see *23*), an understanding of the nature of protein-induced changes in lipid phase behavior may be the key to understand these membrane processes. However, little is known about the mechanism by which proteins affect membrane lipid organization.

In this study we want to investigate in molecular detail how transmembrane proteins are able to modulate lipid phase behavior. This can be conveniently examined by studying the interactions between peptide models of membrane-spanning protein domains and phospholipid model membranes. Especially nonbilayer lipids will be suited for such studies, due to their inherent nonbilayer phase forming propensity. The synthetic phospholipid 1,2-dielaidoylphosphatidylethanolamine (di C18:1_t-PE; DEPE) has been used as a model nonbilayer lipid (*24*−*26*), because it undergoes gel to liquid-crystalline and bilayer to inverted hexagonal (H_{II}) phase transitions at experimentally convenient temperatures of about 37 and 58 °C, respectively (*27*).

Previously, several peptides were shown to trigger changes in the phase behavior of DEPE. Alamethicin induces a cubic phase when incorporated in DEPE (*26*). Gramicidin S causes the formation of an isotropic, probably inverted cubic, phase (*28*). For these peptides, the mechanism was suggested to involve changes in membrane curvature. However, the lack of known and precisely defined peptide orientations prohibited interpretation of the results on a molecular level. The transmembrane channel forming peptide gramicidin A was shown to affect the phase behavior of DEPE in a different way, by promoting the formation of an H_{II} phase (*24*, *29*). Here the mechanism was proposed to be an increase in the volume of the membrane hydrophobic core (*30*). Although gramicidin A does have certain characteristics typical of intrinsic membrane proteins, it is not an ideal model of a membrane-spanning peptide, because it does not adopt an α-helical conformation, and it spans the membrane as a dimer.

Recently, a class of hydrophobic, uncharged α-helical peptides, called the 'WALP' peptides, have been designed (*31*). As with gramicidin dimers, a transmembrane orientation is stabilized by the presence of tryptophan membrane anchors at both ends of the WALP peptides. The effect of incorporation of WALP peptides on the phase behavior of phosphatidylcholine (PC) membranes, which by themselves are unable to form nonlamellar phases, has been characterized to some detail (*31*−*33*). When incorporated at high peptide concentrations into PC model membranes of greater hydrophobic thickness than the peptide hydrophobic length (negative mismatch), WALP peptides induce the formation of nonbilayer phases. An H_{II} phase is induced in the case of a large negative mismatch, and an isotropic phase is observed for a smaller negative mismatch.

Since the WALP peptides can modulate lipid organization, since they form well-oriented transmembrane α-helices (*31*), and since their lengths can be systematically varied, they are useful for understanding peptide influence on lipid phase behavior at the molecular level. As a nonbilayer lipid, DEPE is expected to be more sensitive to the WALP peptides than is phosphatidylcholine. The fact that DEPE adopts an H_{II} phase at high temperature allows investigation of mismatch-induced changes in the tube diameter, which are directly related to changes in the spontaneous curvature of the systems (*4*). In addition, DEPE allows investigation of the intriguing possibility that a positive mismatch (hydrophobic length of the peptide larger than the bilayer thickness) might stabilize a bilayer relative to a nonbilayer phase. To achieve a range of mismatch situations varying from negative to positive, WALP analogues consisting of 14−31 residues were used. Their effects on the DEPE phase behavior were examined by ^{31}P NMR spectroscopy and small-angle X-ray diffraction. It was found that the peptides strongly affect the phase behavior of DEPE even at low concentrations. The type of induced phase was determined by the extent of mismatch, but peptides with lengths longer than the thickness of DEPE did not stabilize the bilayer phase. Molecular mechanisms will be discussed by which a peptide/lipid hydrophobic mismatch can promote the observed changes in lipid organization.

MATERIALS AND METHODS

Materials. 1,2-Dielaidoylphosphatidylethanolamine (DEPE) was obtained from Avanti Polar Lipids Inc. (Birmingham, AL). 2,2,2-Trifluoroethanol (TFE) and trifluoroacetic acid (TFA) were from Aldrich (Milwaukee, WI). Other reagents were of analytical grade. The synthetic peptides used are referred to as WALP*n*, with *n* being the total number of amino acids. The peptide sequences are acetyl-GWWL-$(AL)_i$WWA-ethanolamine, with $i = 3.5$, 4.5, 5, 6, 7, 8, 10, or 12. The WALP peptides were synthesized using previously described methods (*31*,*34*), with one modification. Based on practical considerations, the N-terminal end of the peptides was modified from a formylated alanine to an acetylated glycine (*35*). Control experiments showed no significant differences between peptides with either N-terminus when incorporated in DEPE model membranes.

^{31}P NMR Sample Preparation. The peptides were incorporated into the phospholipid membranes, using a previously described procedure (*31*). A lipid film consisting of 30 μmol of DEPE was obtained from a stock solution in chloroform after removal of the solvent using a rotavapor and further drying under vacuum. The lipid was then hydrated with 0.5 mL of distilled water, and dispersed by rigorous vortexing at around 40 °C, where DEPE is in the liquid-crystalline bilayer (L_α) phase. The peptide was dissolved in up to 100 μL of TFA, quickly dried under a flow of nitrogen, and dissolved in 1.0 mL of TFE. To remove residual TFA, the peptide was dried on a rotavapor, and again dissolved in 1.0 mL of TFE. After determination of the concentration by measuring the absorbance at 280 nm, and further dilution as required, 0.5 mL of peptide solution in TFE was added to the hydrated lipid. To mix the peptide and lipid, the sample was vortexed rigorously. Next, approximately 10 mL of distilled water was added, and the sample mixture was lyophilized. The dried sample was then transferred to a 7.5 mm diameter Pyrex tube, and hydrated with approximately 1.5 mL of buffer (100 mM NaCl, 25 mM Tris-HCl, 1 mM EDTA, pH 7.4). The tubes were centrifuged for 15 min at 27000*g*, to spin down the membranes. The supernatant liquid was removed, and the spun down material was resuspended in approximately 1.5 mL of buffer. Typically a total of three such centrifugation steps were done. After the final centrifugation step, the supernatant was not removed completely,

but was kept at a volume approximately equal to the pellet size to ensure full hydration of the sample. The resulting NMR sample was stored under nitrogen. To fully homogenize the peptide/lipid mixture, it was freeze−thawed approximately 15 times, by subsequent freezing in a CO_2/ethanol bath and thawing at about 40 °C. Before the actual NMR measurements, the samples were further equilibrated by slowly cycling them 3 times over the temperature range between 20 and 60 °C, over a period of approximately 1 h per cycle.

^{31}P NMR Measurements. The ^{31}P NMR measurements were performed on a Bruker MSL 300 spectrometer, at 121.5 MHz, as described previously (*31*). Between 1500 and 5000 free induction decays were accumulated. An exponential multiplication was applied before the Fourier transformation, resulting in a 100 Hz line-broadening. All spectra were scaled to the same height for plotting. Since multiphasic ^{31}P NMR spectra are basically summations of the signals of lipids in the different phases, it was possible to determine the amount of each phase by subtracting spectra obtained for samples containing a single type of phase from spectra showing signals from multiple lipid phases. Subsequently, the percentage of each phase could be determined by comparing peak areas before and after subtraction. The experimental error in these percentages was estimated to be 5%.

Small-Angle X-ray Measurements. Small-angle X-ray measurements were performed on samples that had been characterized by ^{31}P NMR. Following the recording of the ^{31}P NMR spectra, the buffer was replaced by water in several centrifugation steps by removing the supernatant and dispersing the samples in water. Next, the rinsed sample was lyophilized from water. The samples were rehydrated in a small excess of water, cycled several times between 20 and 60 °C, pelleted, and transferred with some excess water into 1 mm glass capillaries. Small-angle X-ray diffraction experiments were carried out with an 18 kW Rigaku Rotaflex RU300 rotating anode generator and a 2D Marresearch imaging plate detector with a plate diameter of 180 mm and a pixel size of 150 μm × 150 μm. Monochromatic Cu K_α radiation ($\lambda = 1.54$ Å) was achieved by a flat germanium (111) crystal. The spot size, defined by three sets of vertical and horizontal slits, was approximately 0.8 mm × 0.8 mm. Temperature variations (±1 °C) were done by increasing the temperature. Peak positions were accurately determined by Gaussian fits after background subtraction. The obtained repeat distances were used to calculate the H_{II} phase tube diameters using the equation:

$$\text{tube diameter} = \text{repeat distance} \times 2/\sqrt{3}$$

RESULTS

WALP16 in DEPE. ^{31}P NMR and small-angle X-ray diffraction were used to study the phase behavior of DEPE dispersions in the absence and presence of the WALP peptides. As illustrated in Figure 1A, upper row, DEPE without peptide at 30 °C gives a ^{31}P NMR spectrum with a high-field peak and low-field shoulder, typical of lipids organized in a bilayer (*36*, *37*). The broadness is indicative of a gel phase. At 40 and 50 °C, the ^{31}P NMR spectrum retains a high-field peak and a low-field shoulder; the smaller line width is indicative of a liquid-crystalline bilayer. At 60 °C, a spectrum typical for an H_{II} phase is observed, with a low-field peak, a high-field shoulder, and a width reduced by a factor of 2. The temperature dependence of the ^{31}P NMR spectra was found to be consistent with previously published transition temperatures of DEPE of approximately 37 °C for the gel to liquid-crystalline transition temperature (T_L), and 58 °C for the liquid-crystalline to H_{II} phase transition temperature (T_H) (*27*).

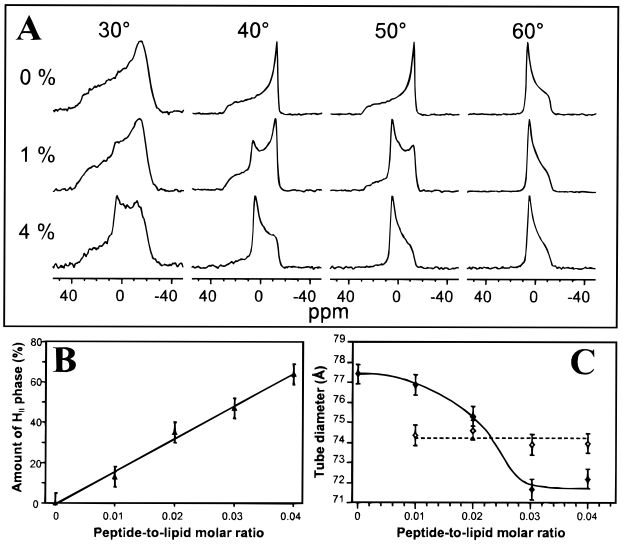

FIGURE 1: Effect of WALP16 on DEPE polymorphism. (A) ^{31}P NMR spectra of DEPE liposomes containing 0, 1, and 4 mol % WALP16, measured at 30, 40, 50, and 60 °C. (B) Amount of WALP16-induced H_{II} phase at 40 °C as a function of peptide concentration. The line represents a linear fit to the data. (C) Hexagonal phase tube diameters determined by small-angle X-ray diffraction for the DEPE/WALP16 system at 40 °C (open symbols, dashed line) and 60 °C (filled symbols, solid line) as a function of peptide concentration.

Figure 1A also shows ^{31}P NMR spectra of DEPE samples containing 1 and 4 mol % WALP16 (with respect to lipid). Even at the lowest peptide concentration (1 mol %), a significant promotion of H_{II} phase formation is observed. At 40 and 50 °C, the NMR spectrum consists of a combination of components representative of an L_α phase and an H_{II} phase. The presence of 4 mol % WALP16 results in larger amounts of H_{II} phase at all temperatures. Also below the regular gel to liquid-crystalline transition temperature, a small H_{II} phase component is observed.

Figure 1B shows that the amount of WALP16-induced H_{II} phase at 40 °C, as determined from the ^{31}P NMR data, is linearly dependent on the peptide concentration. The efficiency of H_{II} phase formation is similar to that found previously for gramicidin A in DEPE (*29*). A linear fit of the data suggests that approximately 6 mol % WALP16 would be sufficient to obtain a pure H_{II} phase at 40 °C.

The ^{31}P NMR data suggest that WALP16 induces the formation of an H_{II} phase at 40 °C with a well-defined and constant peptide/lipid ratio. This was supported by small-angle X-ray diffraction experiments. Figure 1C shows the evolution of the hexagonal phase tube diameters obtained of the WALP16/DEPE system at 40 and 60 °C as a function of peptide concentration (selected diffraction patterns will be shown below). At 60 °C, where all lipids are in the H_{II} phase, the tube diameter decreases steadily with increasing amount of WALP16 up to 3 mol %, where it appears to reach a minimum. In contrast, at 40 °C, where the amount of H_{II}

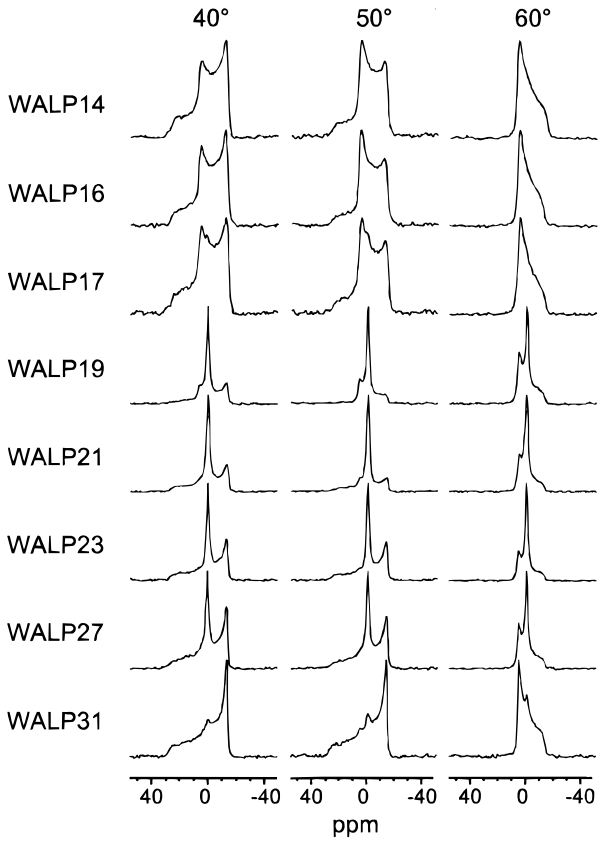

FIGURE 2: ^{31}P NMR spectra of DEPE model membranes containing 2 mol % WALP peptides, at 40, 50, and 60 °C.

phase increases with increasing peptide concentration, the tube diameter stays about constant at ~74.2 Å, independent of the amount of WALP16. The same tendency is observed at 40 °C for the lamellar repeat distance of ~54.5 Å, that is identical to the one of pure DEPE and stays constant for all peptide concentrations investigated. These results suggest the coexistence at 40 °C of a peptide-depleted lamellar phase and a peptide-rich H_{II} phase with a well-defined stoichiometry, similar to that suggested previously for gramicidin A in DEPE (*24*).

^{31}P NMR Study of WALP/DEPE Mismatch. To study the effect of hydrophobic mismatch, WALP analogues with varying hydrophobic lengths were incorporated into DEPE model membranes at a peptide concentration of 2 mol %. Figure 2 shows the results of ^{31}P NMR measurements on these peptide/lipid mixtures at 40, 50, and 60 °C, where we focus on the effect of the peptides on the L_α and H_{II} phases of pure DEPE. The percentages of the different phases observed in these spectra were determined as described under Materials and Methods. These percentages are shown in Figure 3 at 40 °C, below T_H, and at 60 °C, above T_H.

The shortest peptides used are WALP14, WALP16, and WALP17. At temperatures of 40 and 50 °C, DEPE by itself forms a bilayer, but in the presence of these short peptides, a combination of both an L_α phase and a peptide-induced H_{II} phase is observed. The amount of induced H_{II} phase is about the same for each of these peptides (~30%). Above T_H, at 60 °C, a pure hexagonal phase is observed, similar as for the pure lipid. With these peptides, no phases other than bilayer and inverted hexagonal were observed.

Peptides of 'intermediate' and longer length have strikingly different behavior (Figures 2 and 3). Below T_H, at 40 and

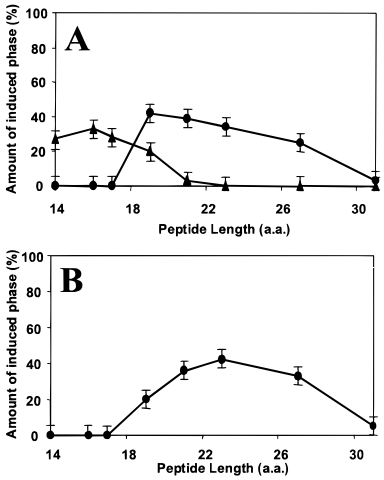

FIGURE 3: Signal intensities from ^{31}P NMR spectra were used to calculate the relative amounts of induced nonbilayer phases, for samples containing the various WALP peptides. At 40 °C, DEPE adopts the L_α phase, with induced isotropic (circles) and H_{II} (triangles) phases as shown in panel A. At 60 °C, DEPE is in the H_{II} phase, with an induced isotropic phase (circles) as shown in panel B.

50 °C, for WALP19 and WALP21, a complex situation is observed, with a large amount of isotropic phase and small amounts of both L_α and H_{II} phase. For the longer peptides WALP23 and WALP27, at these temperatures only an isotropic phase coexisting with the L_α phase is observed. The amount of isotropic phase in these samples decreases with peptide length (Figure 3A), until finally only a minor isotropic signal is observed in the presence of the longest peptide, WALP31. Above the L_α to H_{II} transition, at 60 °C, in all cases two components are observed: the H_{II} phase, and an isotropic signal. Here, the isotropic component initially increases in intensity relative to the H_{II} component, to an apparent maximum near WALP23, and then it decreases again with increasing peptide length (Figure 3B). Samples containing WALP31 again only have a minor isotropic signal, thereby showing essentially the same phase behavior as pure DEPE.

Small-Angle X-ray Diffraction Study of the Phase Behavior of WALP/DEPE. After the ^{31}P NMR measurements, small-angle X-ray analysis (SAX) was performed on the samples. Figure 4 shows selected diffraction patterns of pure DEPE and WALP/DEPE mixtures at 60 °C. In all cases, the X-ray experiments further confirmed the phase behavior of the WALP/DEPE systems obtained by ^{31}P NMR. Induction of an H_{II} phase, coexisting with a lamellar phase, was observed below T_H for the shorter peptides, WALP14 through WALP21, while no H_{II} phase induction was observed under these conditions for WALP23 or longer peptides (data not shown). In the case of the intermediate and longer peptides (WALP19 to WALP27), where the ^{31}P NMR data show peptide-induced formation of an isotropic phase, a weak diffraction peak was observed that could not be attributed to either the L_α or the H_{II} phase, suggesting that the isotropic phase may be a cubic one. To verify the latter, a DEPE sample containing 4 mol % WALP23 was prepared, where at 60 °C the isotropic phase is the only phase observed. The X-ray diffraction pattern of this phase indeed corresponds to a cubic phase (Figure 4C). Diffraction peaks are spaced in the ratios $\sqrt{2}$: $\sqrt{3}$: $\sqrt{4}$: $\sqrt{6}$: $\sqrt{8}$: $\sqrt{9}$, consistent with a *Pn3m* double diamond cubic

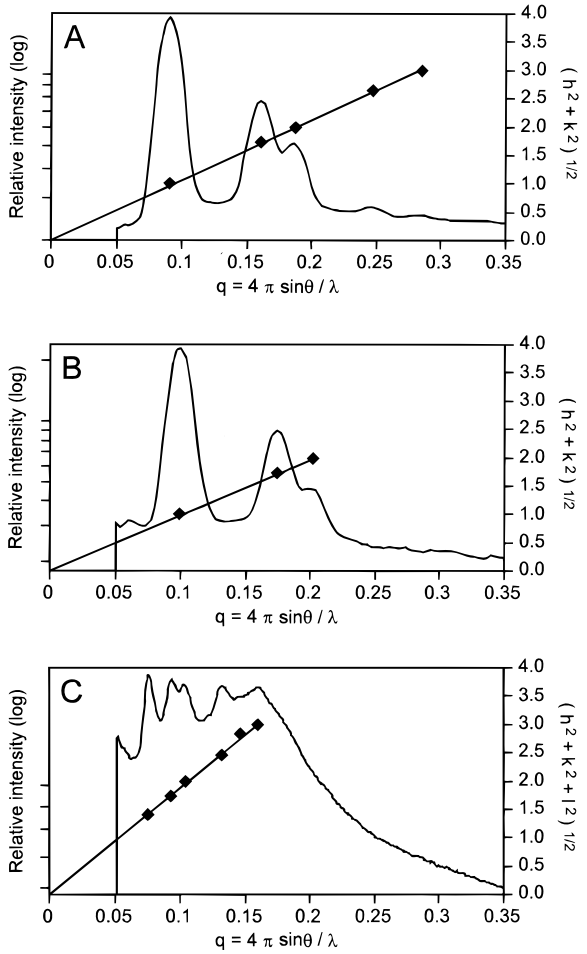

FIGURE 4: Small-angle X-ray diffraction patterns obtained at 60 °C for the hexagonal phases of pure DEPE (A) and DEPE containing 4 mol % WALP16 (B) and for the *Pn3m* cubic lattice of DEPE containing 4 mol % WALP23 (C). The $(h^2 + k^2 + l^2)^{1/2}$ for *hkl* indices (with $l = 0$ for the hexagonal lattices) versus reciprocal spacings fall on straight lines. The lattice constants obtained as the reciprocal slope are 67.0 Å (A), 62.5 Å (B), and 118.8 Å (C).

space group having a lattice constant of ~119 Å. This is similar to the alamethicin-induced *Pn3m* cubic phase of DEPE at 60 °C (*26*).

Lattice Constants as a Function of Peptide Length. Figure 5 shows the tube diameters of the H_{II} phases at 40 and 60 °C of DEPE containing 2 mol % WALP peptides obtained from the X-ray data. At 40 °C, where a peptide-induced H_{II} phase is found for WALP14 to WALP21, the tube diameter increases linearly with peptide length up to WALP19 (Figure 5A). Upon increasing the peptide length from WALP19 to WALP21, the tube diameter does not further increase and stays approximately constant at a value that is somewhat larger than that of pure DEPE at 60 °C. The coexisting lamellar phase at 40 °C that is observed for all peptides (data not shown) has a constant repeat distance of about 54.5 Å.

At 60 °C, where an H_{II} phase is observed independent of the peptide length, a similar trend is observed (Figure 5B). Incorporation of the shortest peptide, WALP14, leads to a significant reduction in the tube diameter compared to pure DEPE. The tube diameter increases linearly with peptide length up to WALP19. For the longer peptides, the tube diameter at 60 °C stays about constant but is now slightly smaller than that of pure DEPE. The only exception is

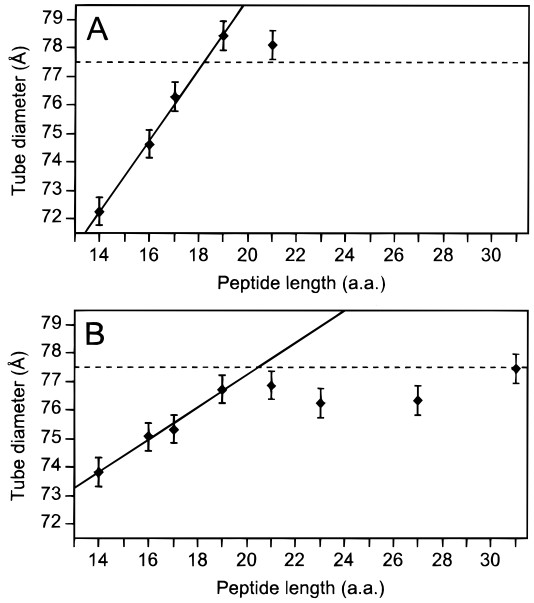

FIGURE 5: Hexagonal phase tube diameters determined using small-angle X-ray diffraction measurements of fully hydrated DEPE samples containing 2 mol % WALP peptides, at 40 °C (A) and 60 °C (B). Solid lines indicate linear regression fits to data for WALP14 to WALP19. The horizontal dashed lines indicate the tube diameter for the pure DEPE inverted hexagonal phase at 60 °C.

WALP31 that appears to have no effect on the tube diameter.

The main difference between the systems at 40 and 60 °C is the steeper slope, or the more pronounced effect of the peptide length on tube diameter, at 40 °C. This is attributed to a higher local peptide concentration in the peptide-induced H_{II} phase at temperatures below T_H.

Lattice constants for the cubic phase induced by the intermediate and longer peptides could not be determined accurately due to the biphasic or triphasic nature of the samples containing 2 mol % WALP peptides.

DISCUSSION

In this study it is shown by ^{31}P NMR and X-ray diffraction experiments that synthetic transmembrane α-helical peptides at 1−2 mol % concentration can have profound effects on the phase behavior of DEPE. The WALP peptides are shown to induce nonlamellar phases, with the type of phase dependent on the extent of mismatch between peptide and lipid. Very short peptides induce formation of an H_{II} phase at temperatures below T_H, and longer peptides induce the formation of a cubic phase. The longest peptide, WALP31, has hardly any effect on the phase behavior of DEPE. An explanation could be that its larger length causes a reduced incorporation in the DEPE system and/or the formation of aggregates, as will be discussed below.

The systematic variation of the WALP peptide length, together with the observation that the WALP peptides form well-oriented transmembrane α-helices (*31*), allows for a detailed examination of their mode of action.

Length of Peptides and Hydrophobic Thickness of the Lipid. To understand how the nonbilayer phase induction depends on the peptide length, one should have estimates of the hydrophobic thickness of both the DEPE and the membrane-spanning part of the peptides.

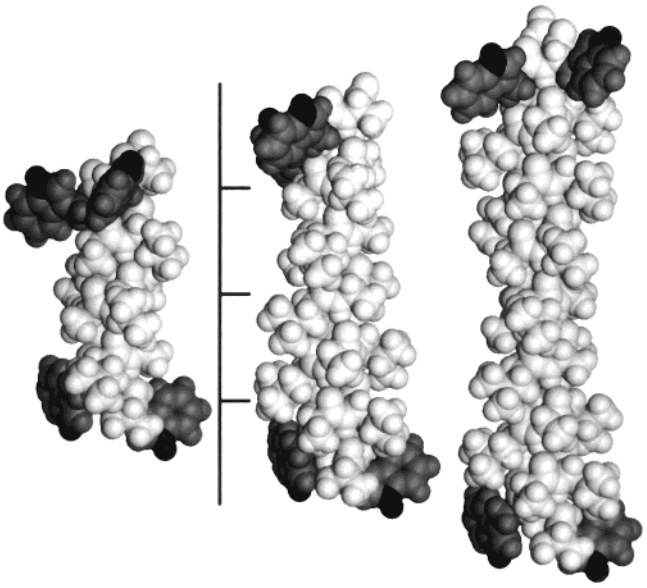

FIGURE 6: Molecular models of the WALP16, WALP23, and WALP31 peptides (from left to right) obtained using Insight II v.98.0 (Molecular Simulations Inc., San Diego, CA). Tryptophans are colored gray, and their indole NH's are black. The (χ_1, χ_2) values of the tryptophans were set to (97, −66) for $Trp^{2,3}$, and to (−150, −60) for $Trp^{n-2,\ n-1}$, to get the indole NH's pointing outward. Models were then refined using Discover (MSI, San Diego, CA). Bars at 10 Å intervals are shown on a 40 Å scale.

To estimate the dimensions of the WALP peptides, molecular modeling was used. Three peptides (WALP16, -23, and -31) were modeled as standard α-helices. The tryptophans were rotated such that the NH of each indole ring was oriented toward the membrane/water interface, in accordance with their suggested role as 'membrane interface anchors' (*38*−*42*). The resulting models were energy minimized and are shown in Figure 6. In these model structures, the distances between the protons of the inner pair and the outer pair of indole NH groups were determined. Also, the distance between the C_α atoms of the outermost C- and N-terminal amino acids was estimated,[2] as well as the length of the hydrophobic stretch of leucines and alanines inside the tryptophans (see Table 1).

DEPE by itself forms an L_α phase at low temperatures and an H_{II} phase at higher temperatures. No detailed data on the dimensions of these phases have been published for DEPE, but they are available for dioleoylphosphatidylethanolamine (DOPE). Although these values will be somewhat larger for DEPE, which has a trans instead of a cis double bond, they will be useful to estimate peptide/lipid mismatch in the DEPE systems. For DOPE in the L_α phase, in excess water, a total bilayer thickness has been reported of 37 Å (*43*). Subtraction of an estimated headgroup thickness of about 11 Å (*44*) leaves a minimal hydrophobic core thickness of about 26 Å for DEPE. The dimensions are significantly smaller in the H_{II} phase. Here, the interaxial bilayer thickness for DOPE is 32 Å (*45*), leaving an estimated hydrophobic core thickness of about 21 Å, which is in fair agreement with the reported value of 20 Å (*46*).

[2] The blocking *N*-acetyl and *C*-ethanolamine groups are expected to have high rotational mobility (*56*) and are relatively hydrophilic, so they contribute little to the hydrophobic length of the WALP peptides.

Table 1: Estimated Dimensions of WALP*n* Peptides of the Sequence Acetyl-GWWL$(AL)_i$WWA-ethanolamine, in Which *n* Is the Total Number of Amino Acids ($n = 2i + 7$)[a]

peptide	Leu-Ala: $C_\alpha-C_\alpha$	terminal $C_\alpha-C_\alpha$[b]	inner Trp	outer Trp
WALP14	10.4	19.3	20.2	23.2
WALP16	13.4	22.3	23.2	26.2
WALP17	14.9	23.8	24.7	27.7
WALP19	17.9	26.8	27.7	30.7
WALP21	20.8	29.7	30.6	33.6
WALP23	23.8	32.7	33.6	36.5
WALP27	29.7	38.6	39.5	42.5
WALP31	35.6	44.6	45.4	48.4

[a] Given are distances between specific atoms in the modeled peptides: the C_α carbons of the beginning and end of the Leu-Ala sequence between the tryptophans [residues 4 to ($n - 3$)], the C_α carbons of the terminals (residues 1 to *n*), and the indole NH hydrogens of the inner and outer pair of tryptophans [residues 2 to ($n - 1$) and 3 to ($n - 2$)]. All distances are in angstroms. [b] The actual total backbone length of the peptides is slightly larger than these ($C_\alpha-C_\alpha$) values due to their (mobile) terminal groups, which were not modeled.

From comparing the dimensions of the peptides and lipid, it can be concluded that the total length of the shortest peptide will be considerably smaller than the hydrophobic thickness of DEPE. For the longest peptides, even the length of the hydrophobic stretch of leucine and alanine between the tryptophans will be significantly larger than the hydrophobic part of DEPE in the L_α phase. Therefore, it can be concluded that our systems cover a wide range of mismatch situations, varying from negative (peptide too small) to positive (peptide too large).

Induction of Inverted Hexagonal Phase. As indicated above, the different peptides have differing extents of (mis)-matching with the liquid-crystalline bilayer of the pure lipid. The peptide/lipid system reacts to this situation by inducing the formation of either an H_{II} phase or an isotropic (cubic) phase. We will first discuss peptide-induced H_{II} phase formation, starting with the shortest peptides.

The shortest peptides, WALP14, WALP16, and WALP17, have a total C_α to C_α distance (19−24 Å) that is shorter than the hydrophobic thickness of the DEPE bilayer (>26 Å). Besides the overall length as indicated by the $C_\alpha-C_\alpha$ distance, the tryptophan−tryptophan distances are also of interest. While tryptophans have a preference for the headgroup region, these peptides are so short that it is impossible to simultaneously maintain the transmembrane α-helix and position all of the tryptophans in the interfacial regions of the lamellar phase. Therefore, both the total peptide length and the tryptophan positions indicate a significant negative mismatch of these short peptides with the L_α phase. It was found that all three peptides promote H_{II} phase formation below the T_H of DEPE. The experimentally observed reduction in the tube diameter suggests that these peptides have a negative spontaneous curvature effect on the lipid that is directly proportional to the length of the peptide. This is consistent with the idea that the peptides are located mostly in the hydrophobic core of the H_{II} phase where they would increase the hydrophobic volume of the system and create additional space between the headgroups, thereby allowing an increased curvature for the lipids with decreasing peptide length. Such a model would be consistent with a recently proposed theoretical model of the $L_\alpha-H_{II}$ phase transitions induced by short transmembrane peptides (*47*). The suggested location of the peptides is shown schematically in Figure 7.

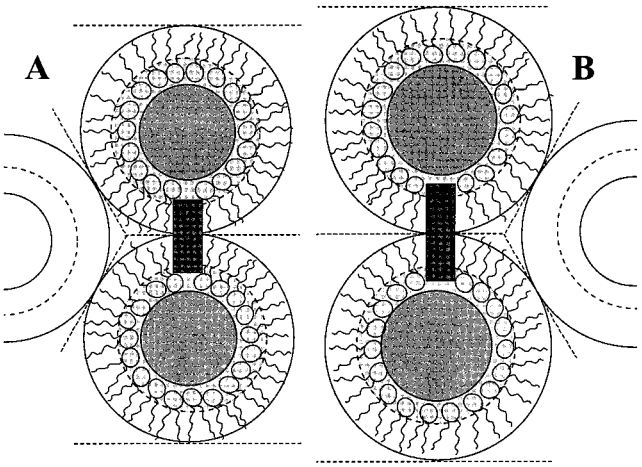

FIGURE 7: Schematic drawing of cross sections showing parts of inverted hexagonal phases with imbedded peptides. The peptides are shown as dark boxes. The shortest peptide in (A) reduces the tube diameter by allowing more space between the lipid headgroups than does the intermediate length peptide in (B). Longer peptides probably do not fit well in the H_{II} phase, and were found to induce a cubic phase.

This figure illustrates how the shortest peptides could take up less space in the headgroup area, resulting in a decrease in tube diameter.

Below T_H, the relative amount of H_{II} phase induced by WALP16 increases linearly with peptide concentration, but its dimensions stay constant (Figure 1B,C). These findings are indicative of a well-defined lipid-to-peptide ratio in the H_{II} phase. One may imagine that the lipids arrange themselves around a lattice imposed by the peptide itself, located at the shortest distance between neighboring tubes (see also ref *31*). This would effectively take care of the mismatch, since the smaller lattice of the H_{II} phase would allow all tryptophans of these peptides to interact with the interface region. Such an arrangement might in addition stabilize the H_{II} phase by partially relieving acyl chain packing constraints, which arise from the requirement for a nonuniform effective length of the acyl chains around the tubes in this phase (*1*). Together, the results indicate that these shorter peptides effectively partition into the H_{II} phase below T_H. Consistent with this, we find experimentally that none of these peptides has any effect on the lamellar repeat spacing of DEPE in the L_α phase at 40 °C, indicating that the persisting lamellar phase is essentially depleted of peptide.

When the temperature is raised above T_H for DEPE with WALP14 through WALP17, the system is monophasic, and consists only of H_{II} phase. In this case, as was shown for WALP16, the tube diameter of the peptide-containing H_{II} phase decreases with increasing peptide concentration (Figure 1C). Thus, the peptide now mixes with all lipids in the H_{II} phase, thereby changing the lattice with increasing peptide concentration until a minimum tube diameter is obtained. The above is probably also true for the other short peptides, WALP14 and WALP17. In all cases, at 40 °C the systems are biphasic with the H_{II} phase containing essentially all of the peptide and with dimensions imposed by the peptide, whereas at 60 °C the peptides dilute in the H_{II} phase of DEPE. This would explain the steeper slope of the reduction of the tube diameter with peptide length at 40 °C as compared to 60 °C (Figure 5).

When the peptide length is increased to WALP19 and WALP21, decreasing amounts of H_{II} phase are formed below T_H. WALP19 and WALP21 have total lengths of about 27−30 Å, which is close to, or slightly larger than, the hydrophobic thickness of the bilayer (>26 Å). Also the tryptophans of these peptides are located in the bilayer interface region. Yet these peptides are still significantly shorter than the total bilayer thickness (>37 Å).

In contrast to the situation for the shortest peptides, for WALP19 through WALP27 effectively the same tube diameters are found in the H_{II} phase at 60 °C (Figure 5). It is possible that in these cases hydrocarbon packing constraints prevent further increases in tube diameter, and that these longer peptides adapt by 'tilting' or 'kinking' in the H_{II} phase. It should be realized, however, that it is increasingly unfavorable for longer peptides to be accommodated in the H_{II} phase, since these peptides induce a significant amount of isotropic phase (see below). Indeed, the longest peptide, WALP31, may be excluded from both the bilayer and the H_{II} phase. This is supported by the observation that neither the bilayer repeat distance nor the H_{II} tube diameter is affected by the presence of this peptide.

Energetic Considerations. The type of phase formed by a lipid under specific conditions is determined by the relative magnitudes of two counteracting energy components. First of all, the lipids have a certain inherent curvature. This curvature is determined by the relative sizes of the hydrated headgroup and the lipid chains. Phosphatidylethanolamines have an inherent negative curvature, due to a small headgroup. Forcing these lipids into a flat lamellar phase leads to a certain *bending energy*, favoring the formation of inverted phases such as the H_{II} phase. Second, the lipids in the lamellar phase are arranged in monolayers of uniform thickness, but in the H_{II} phase they are forced into monolayers of changing thickness. This increases the energy of lipids in the H_{II} phase. This so-called *interstitial energy* therefore counteracts the bending energy. Both energies are dependent on the temperature of the system. At the L_α to H_{II} phase transition temperature, the bending and interstitial energies are balanced, allowing the transition to occur. Below this temperature, the larger interstitial energy prevents the formation of the hexagonal phase.

The presence of the WALP peptides changes the energetics of the lipid phase transition. In addition to the above-mentioned energies governing the behavior of the lipids themselves, a new energetic component has been added. The interaction energy of the peptide with the lipid is dependent upon the lipid environment. This energy is dominated by the preference of the peptide's hydrophobic residues for the hydrophobic core of the bilayer, combined with the preference of the tryptophans for a location within the lipid interface.

To estimate the energies, one has to combine theory and measurements. This involves combining equations to calculate the two energies (eqs 3 and 7 from ref *48*) with experimental results for tube diameter, intrinsic monolayer curvature, and bending modulus (Figures 2 and 5 from ref *49*). These data are available for DOPE, but not for DEPE. For DOPE, an estimate was obtained of a net energy difference between the L_α and the H_{II} phase of $\sim 7 \times 10^{-12}$ J per meter of tube length. With an estimated 20 lipids per circumference and an approximate lipid area of 60 Å^2, this

would give ~0.2 kJ/mol energy difference between the two phases. These estimates were obtained at ~0 °C, at which temperature DOPE is close to the halfway point between the $L_\beta \rightarrow L_\alpha$ and $L_\alpha \rightarrow H_{II}$ transition temperatures. For DEPE, a similar halfway point occurs at 45 °C. The results show that at this temperature the shortest peptides induce a hexagonal phase in DEPE, in which per peptide molecule ~14 lipids are present (~28% H_{II} phase at a 1/50 P/L ratio). Thus, extrapolating the energetics obtained for DOPE to the situation for DEPE, the presence of 1 peptide would correspond to an energy difference of ~3 kJ/mol for the ~14 lipids it affects. This energy is small compared to the energy of a single hydrogen bond.

It might be tempting to ascribe the effect of the peptides to the hydrogen bonding by the tryptophan's indole N−H protons, but these contribute only partially to the tryptophan's interfacial preference. Modified tryptophans that are unable to hydrogen bond still display a preference for an interfacial location (*39*).

Although these energetic factors are important in determining the phase transition, one should keep in mind that kinetic factors also play a role. Specifically, kinetic reasons have been implicated in preventing the formation of cubic phases in PE systems (*50*). The peptides change not only the energetics of the phase transition, but also its kinetics. This could be especially important for the longer peptides, which were found to induce a cubic phase.

Induction of Isotropic (Cubic) Phase. In addition to inducing a small amount of H_{II} phase, WALP19 and WALP21 induce a significant amount of isotropic phase. Also the longer peptides, WALP23 and WALP27, induce an isotropic phase, but these peptides do not promote H_{II} phase formation. For WALP23, the isotropic phase could be identified by X-ray diffraction as a *Pn3m* cubic phase (Figure 4C). It is likely that also for the other peptide/lipid systems this isotropic phase represents a cubic phase. First, in phase diagrams such a cubic phase is generally found between an L_α and an H_{II} phase, as observed in the present study. In all cases, it showed a strong hysteresis (the samples required freezing to remove the isotropic signal), as is characteristic of the cubic phase. Furthermore, in all samples in which ^{31}P NMR showed an isotropic signal, a weak X-ray reflection was observed (data not shown), that could not be attributed to an L_α or H_{II} phase. Finally, the induction of a cubic phase has been observed previously in DEPE, by alamethicin (*26*), in the presence of DMPE with a PEG550 chain covalently attached to its headgroup (*51*), and after rapid temperature cycling (*52, 53*).

Let us first discuss the peptide-induced formation of a cubic phase for the intermediate length peptides WALP19 through WALP23. These peptides would be still shorter than the total bilayer thickness (>37 Å), and have their tryptophans located at the interface below the phosphates. The formation of a cubic phase upon incorporation of these peptides could be due to mismatch-induced effects on the lipid spontaneous curvature. DEPE itself has a negative spontaneous curvature. While the shortest peptides, WALP14 through WALP17, will further increase this negative curvature, thereby promoting H_{II} phase formation, incorporation of longer peptides might progressively decrease the spontaneous curvature of the system, thus favoring the formation of a cubic phase relative to an H_{II} phase. Why would this then occur below $T_{H\alpha}$? It has been suggested that the L_α to H_{II} phase transition of DEPE involves intermediate lipid structures which could evolve either to a cubic or to an H_{II} phase, depending on the circumstances, but that in pure DEPE the formation of an H_{II} phase is kinetically favored (*50*). Similar to what has been proposed for the DEPE/alamethicin system (*26*), the longer peptides might perturb the DEPE bilayer enough to relieve the kinetic hindrance [e.g., by lowering the bilayer rupture tension (*50*)] of forming the lower energy cubic phase, which would then trigger the induction of nonlamellar structures below T_H.

At $T < T_H$, as the peptide length increases from WALP19 through WALP23, the peptides will better match the bilayer thickness in the L_α phase, and partitioning into the bilayer will become less unfavorable. This may explain the slight decrease of the amount of isotropic phase with peptide length. In the cubic phase, the hydrophobic 'bilayer' thickness can be expected to be smaller than in an L_α phase and larger than in an H_{II} phase. Above T_H, a bilayer is no longer present, and partitioning of these intermediate length peptides in the isotropic phase will thus be increasingly more favorable than in the H_{II} phase. Therefore, in this case the amount of isotropic phase may be expected to increase with peptide length from WALP19 to WALP23, as indeed was observed.

The still longer peptide WALP27 has a total length of about 39 Å that is slightly exceeding the total thickness of the bilayer (>37 Å). In the modeled conformation, this peptide would have its tryptophans so far apart that they would be slightly outside the headgroup region if the peptide would span the membrane with the helix axis parallel to the membrane normal. Normally, when a peptide is longer than the lipid, one would expect it to induce a positive spontaneous curvature on the system. However, given the negative spontaneous curvature of DEPE alone, WALP27 might lead to a smaller negative curvature, thereby inducing the H_{II} to cubic phase transition. Below T_H, WALP27 could be expected to prefer partitioning into the bilayer relative to the cubic phase, more so than its shorter analogues. This would lead to a further decrease in the amount of isotropic signal, which was indeed observed. However, also at $T > T_H$, the amount of isotropic phase relative to the H_{II} phase appears to decrease slightly for WALP27 relative to WALP23, which would be counter to the trend below T_H. A possible explanation is that WALP27 may be rather long to fit well into either the cubic phase or the L_α phase, and that as a response it could partially aggregate or not fully associate with the lipid. Indeed the longest peptide, WALP31, does not significantly affect the lipid's phase behavior and is most likely not incorporated into the bilayer due to the large positive mismatch (see below).

Lack of Bilayer Stabilization by Longer Peptides. An important observation was that a positive mismatch did not lead to bilayer stabilization. Even in the presence of the longest peptides, no L_α phase was observed at temperatures above T_H. Yet it is known that lysophosphatidylcholine, which has a positive spontaneous curvature, can counteract the negative spontaneous curvature of phosphatidylethanolamine and stabilize bilayer formation (*54*). Apparently this does not happen for a positive curvature induced by peptide/lipid mismatch. Instead, the longest peptide, WALP31, appears to react to the mismatch by not incorporating in the membrane. Such behavior was recently demonstrated by

sucrose density gradient centrifugation experiments for WALP31 in mixtures of DOPE and dioleoylphosphatidylglycerol (S. Morein, R. E. Koeppe II, G. Lindblom, B. de Kruijff, and J. A. Killian, manuscript submitted), as well as in phosphatidylcholine bilayers (M. R. R. de Planque, E. Goormaghtigh, R. M. J. Liskamp, R. E. Koeppe II, and J. A. Killian, manuscript in preparation). In these cases, the peptides were found to segregate out of the bilayer as peptide-rich aggregates together with a small number of lipids. It is likely that the same behavior occurs for WALP31 in DEPE in the present study, as supported by the lack of effect of this peptide on T_H and the H_{II} tube diameter. The small isotropic signal observed in both the bilayer and H_{II} phases of WAL31/DEPE mixtures may then be representative of lipids in such peptide-rich aggregates.

In contrast to WALP31, the somewhat smaller WALP27 clearly is at least partially associated with the lipids and appears to be present both in the H_{II} phase and in the isotropic phase above T_H. However, also for this peptide no stabilization of the L_α phase was observed. Although it is not known what exactly determines the energies of the peptide/lipid systems in the various phases, it can be concluded from these results that the energy cost of a peptide/lipid positive mismatch in the L_α phase is too high to stabilize the bilayer relative to nonlamellar phases. A possible explanation is that it is more difficult for the lipid/peptide system to adapt to a positive mismatch in an L_α phase than it is in a cubic or H_{II} phase, where the lipids are more disordered and may allow a greater flexibility in either the conformation or the orientation of the peptide.

CONCLUDING REMARKS

In summary, we have shown that transmembrane α-helical peptides of varying lengths are able to efficiently induce the formation of different types of nonlamellar phases in DEPE. The WALP peptides can induce both the formation of an H_{II} phase, at large negative mismatch, and the formation of a cubic phase, at a range of mismatch from slightly negative to positive. Peptides with a large positive mismatch do not stabilize the bilayer, most likely because the energetic cost of accommodating such peptides in the L_α phase is too high.

Previously, effects of negative mismatch have been studied in model membranes of the bilayer-forming lipid PC (*31*). Similar results were obtained, indicating that these are general effects of negative mismatch on lipid organization. A notable difference between the two lipid systems was that much larger peptide concentrations were required in PC than in DEPE. This is consistent with the inherent H_{II} phase forming propensity of PE. In fact, it is exactly as predicted based on a theoretical model (*47*).

The results obtained in this study, together with those obtained in PC, support a possible role of peptide/lipid hydrophobic mismatch in modulating lipid organization in biological membranes. In general, biological membranes have an overall bilayer organization, but contain significant amounts of nonbilayer lipids. Therefore, they have a negative spontaneous curvature, and may be considered as frustrated bilayers. We have shown here that in such a case lipid organization can be strongly influenced by transmembrane peptides in a large range of mismatch situations, from highly negative to even slightly positive. Thus, the results suggest that transmembrane peptides are able to disrupt the bilayer organization in biological membranes, in ways that critically depend on the extent of matching between the peptide length and the bilayer thickness, and on the spontaneous curvature of the lipids. These same types of protein/lipid interactions may play a role in the biological functioning of, for example, signal sequences and fusion peptides, which is believed to involve the transient formation of nonlamellar structures (see, e.g., *23*, *55*). Signal sequences and fusion peptides have lengths that normally would not allow them to completely span the membrane, similar to the shorter WALP peptides. In view of the results obtained here, it would be interesting to see whether and how the optimal functional length of such peptides depends on bilayer thickness and membrane lipid curvature.

ACKNOWLEDGMENT

We thank Prof. Ben de Kruijff for helpful discussions and for critically reading the manuscript.

REFERENCES

1. Cullis, P. R., and de Kruijff, B. (1979) *Biochim. Biophys. Acta 559*, 399−420.
2. Lindblom, G., and Rilfors, L. (1989) *Biochim. Biophys. Acta 988*, 221−256.
3. Seddon, J. M. (1990) *Biochim. Biophys. Acta 1031*, 1−69.
4. Gruner, S. M. (1989) *J. Phys. Chem. 93*, 7562−7570.
5. Wieslander, A., Nordstrom, S., Dahlqvist, A., Rilfors, L., and Lindblom, G. (1995) *Eur. J. Biochem. 227*, 734−744.
6. Rietveld, A. G., Killian, J. A., Dowhan, W., and de Kruijff, B. (1993) *J. Biol. Chem. 268*, 12427−12433.
7. Morein, S., Andersson, A., Rilfors, L., and Lindblom, G. (1996) *J. Biol. Chem. 271*, 6801−6809.
8. Gruner, S. M. (1985) *Proc. Natl. Acad. Sci. U.S.A. 82*, 3665−3669.
9. Tate, M. W., Eikenberry, E. F., Turner, D. C., Shyamsunder, E., and Gruner, S. M. (1991) *Chem. Phys. Lipids 57*, 147−164.
10. Cantor, R. S. (1997) *Biochemistry 36*, 2339−2344.
11. Dan, N., and Safran, S. A. (1998) *Biophys. J. 75*, 1410−1414.
12. Keller, S. L., Bezrukov, S. M., Gruner, S. M., Tate, M. W., Vodyanoy, I., and Parsegian, V. A. (1993) *Biophys. J. 65*, 23−27.
13. Senisterra, G., and Epand, R. M. (1993) *Arch. Biochem. Biophys. 300*, 378−383.
14. Li, L., Zheng, L. X., and Yang, F. Y. (1995) *Chem. Phys. Lipids 76*, 135−144.
15. McCallum, C. D., and Epand, R. M. (1995) *Biochemistry 34*, 1815−1824.
16. Starling, A. P., Dalton, K. A., East, J. M., Oliver, S., and Lee, A. G. (1996) *Biochem. J. 320*, 309−314.
17. Hunter, G. W., Negash, S., and Squier, T. C. (1999) *Biochemistry 38*, 1356−1364.
18. Price, A., Economou, A., Duong, F., and Wickner, W. (1996) *J. Biol. Chem. 271*, 31580−31584.
19. Ahn, T., and Kim, H. (1998) *J. Biol. Chem. 273*, 21692−21698.
20. de Kruijff, B. (1987) *Nature 329*, 587−588.
21. Lindblom, G., and Rilfors, L. (1992) in *Structural and Dynamic Properties of Lipids and Membranes* (Quin, P. J., and Cherry, R. J., Eds.) pp 51−76, Portland Press, London.
22. Siegel, D. P., and Epand, R. M. (1997) *Biophys. J. 73*, 3089−3111.
23. Epand, R. M. (1998) *Biochim. Biophys. Acta 1376*, 353−368.
24. Killian, J. A., and de Kruijff, B. (1985) *Biochemistry 24*, 7881−7890.
25. Tate, M. W., and Gruner, S. M. (1989) *Biochemistry 28*, 4245−4253.

26. Keller, S. L., Gruner, S. M., and Gawrisch, K. (1996) *Biochim. Biophys. Acta 1278*, 241−246.
27. McMullen, T. P., and McElhaney, R. N. (1997) *Biochemistry 36*, 4979−4986.
28. Prenner, E. J., Lewis, R. N., Neuman, K. C., Gruner, S. M., Kondejewski, L. H., Hodges, R. H., and McElhaney, R. N. (1997) *Biochemistry 36*, 7906−7916.
29. van Echteld, C. J. A., van Stigt, R., de Kruijff, B., Leunissen-Bijvelt, J., Verkleij, A. J., and de Gier, J. (1981) *Biochim. Biophys. Acta 648*, 287−291.
30. Killian, J. A. (1992) *Biochim. Biophys. Acta 1113*, 391−425.
31. Killian, J. A., Salemink, I., de Planque, M., Lindblom, G., Koeppe, R. E., II, and Greathouse, D. V. (1996) *Biochemistry 35*, 1037−1045.
32. de Planque, M. R. R., Greathouse, D. V., Koeppe, R. E., II, Schafer, H., Marsh, D., and Killian, J. A. (1998) *Biochemistry 37*, 9333−9345.
33. Morein, S., Strandberg, E., Killian, J. A., Persson, S., Arvidson, G., Koeppe, R. E., II, and Lindblom, G. (1997) *Biophys. J. 73*, 3078−3088.
34. Greathouse, D. V., Koeppe, R. E., II, Providence, L. L., Shobana, S., and Andersen, O. S. (1999) *Methods Enzymol. 294*, 525−550.
35. Goforth, R. L., Crawford, T., van der Wel, P. C. A., Rhodes, N. E., Killian, J. A., and Greathouse, D. V. (1999) *Biophys. J. (Abstr.) 76*, A217.
36. Seelig, J. (1978) *Biochim. Biophys. Acta 515*, 105−140.
37. Cullis, P. R., and de Kruijff, B. (1978) *Biochim. Biophys. Acta 513*, 31−42.
38. Koeppe, R. E., II, Killian, J. A., Greathouse, D. V., and Andersen, O. S. (1998) *Bio. Skr. Dan. Vid. Selsk. 49*, 93−98.
39. Yau, W.-M., Wimley, W. C., Gawrisch, K., and White, S. H. (1998) *Biochemistry 37*, 14713−14718.
40. Persson, S., Killian, J. A., and Lindblom, G. (1998) *Biophys. J. 75*, 1365−1371.
41. Kachel, K., Asuncion-Punzalan, E., and London, E. (1995) *Biochemistry 34*, 15475−9.
42. de Planque, M. R. R., Kruytzer, J. A., Liskamp, R. M., Marsh, D., Greathouse, D. V., Koeppe, R. E., II, de Kruijff, B., and Killian, J. A. (1999) *J. Biol. Chem. 274*, 20839−20846.
43. Gruner, S. M., Tate, M. W., Kirk, G. L., So, P. T., Turner, D. C., Keane, D. T., Tilcock, C. P., and Cullis, P. R. (1988) *Biochemistry 27*, 2853−2866.
44. Lewis, B. A., and Engelman, D. M. (1983) *J. Mol. Biol. 166*, 211−217.
45. Chen, Z., and Rand, R. P. (1998) *Biophys. J. 74*, 944−952.
46. Rand, R. P., and Fuller, N. L. (1994) *Biophys. J. 66*, 2127−2138.
47. May, S., and Ben-Shaul, A. (1999) *Biophys. J. 76*, 751−767.
48. Siegel, D. P. (1993) *Biophys. J. 65*, 2124−2140.
49. Epand, R. M., Fuller, N., and Pandm R. P. (1996) *Biophys. J. 71*, 1806−1810.
50. Siegel, D. P. (1999) *Biophys. J. 76*, 291−313.
51. Koynova, R., Tenchov, B., and Rapp, G. (1997) *Biochim. Biophys. Acta 1326*, 167−170.
52. Veiro, J. A., Khalifah, R. G., and Rowe, E. S. (1990) *Biophys. J. 57*, 637−641.
53. Tenchov, B., Koynova, R., and Rapp, G. (1998) *Biophys. J. 75*, 853−866.
54. Madden, T. D., and Cullis, P. R. (1982) *Biochim. Biophys. Acta 684*, 149−153.
55. Killian, J. A., de Jong, A. M., Bijvelt, J., Verkleij, A. J., and de Kruijff, B. (1990) *EMBO J. 9*, 815−819.
56. Koeppe, R. E., II, Vogt, T. C., Greathouse, D. V., Killian, J. A., and de Kruijff, B. (1996) *Biochemistry 35*, 3641−3648.

BI9922594